Electronic Supplementary Material (ESI) for Dalton Transactions.
This journal is © The Royal Society of Chemistry 2016

Electronic Supplementary Information

Preparation and sensing properties of a nitrogen-rich ferrocene-imidazole-quinoxaline triad decorated by pyrrole

María Alfonso,* Alberto Tárraga,* Pedro Molina*

Table of contents

1. NMR and HRMS spectra.

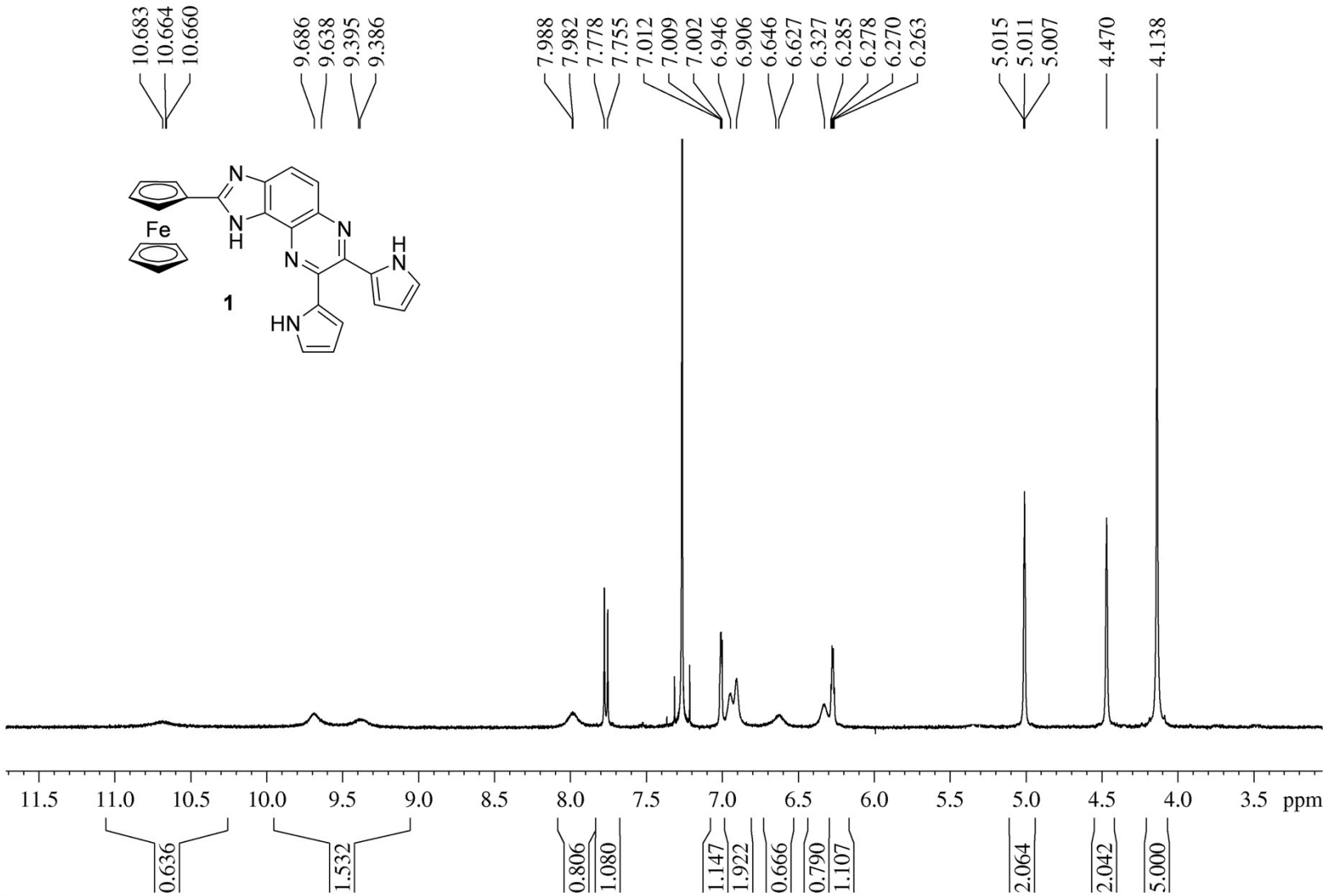

Figure S1. ^{1}H NMR (in $CDCl_3$) spectrum of **1** monitored at 400 MHz.

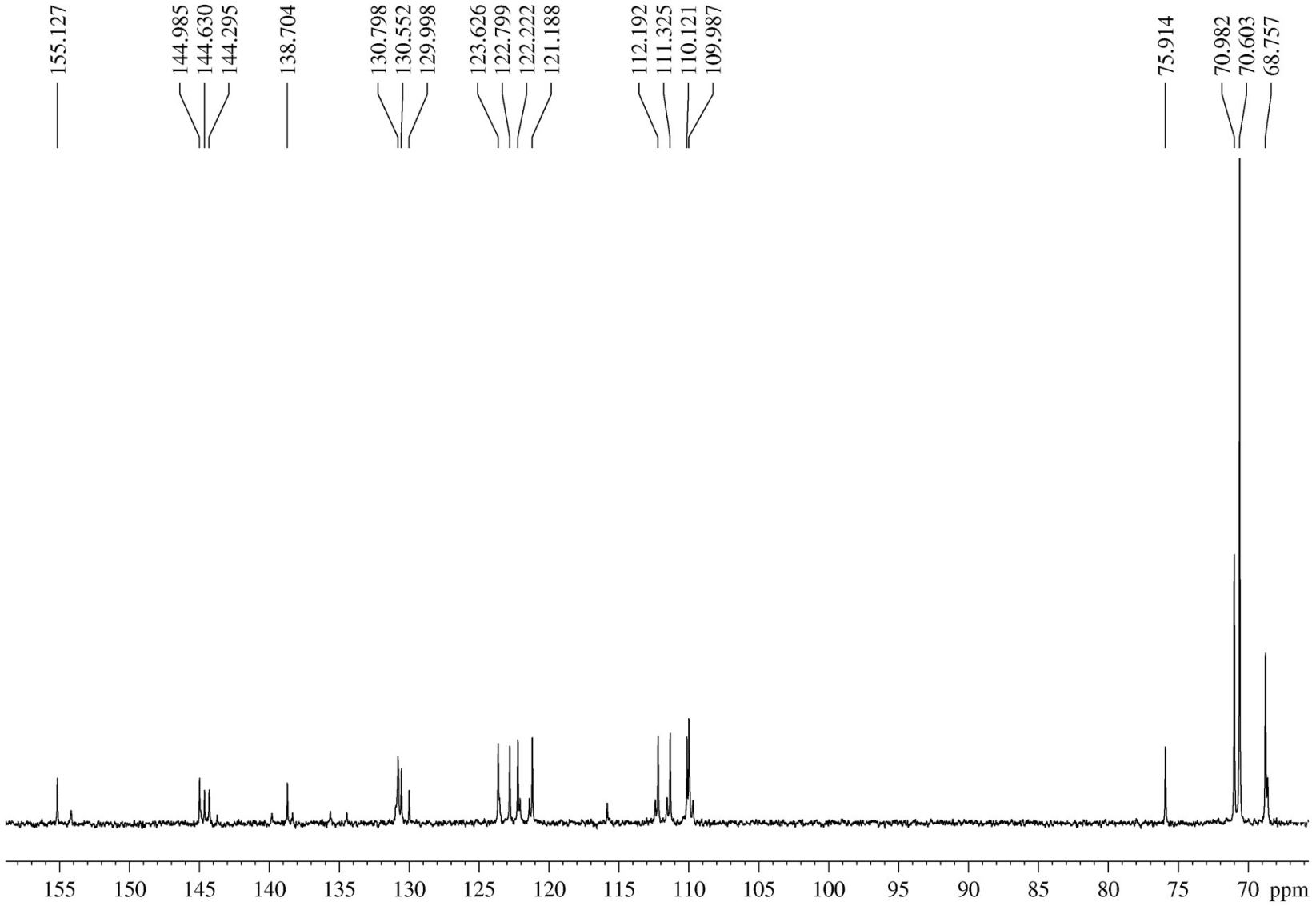

Figure S2. ^{13}C NMR (in DMF-d_7) spectrum of **1** monitored at 400 MHz.

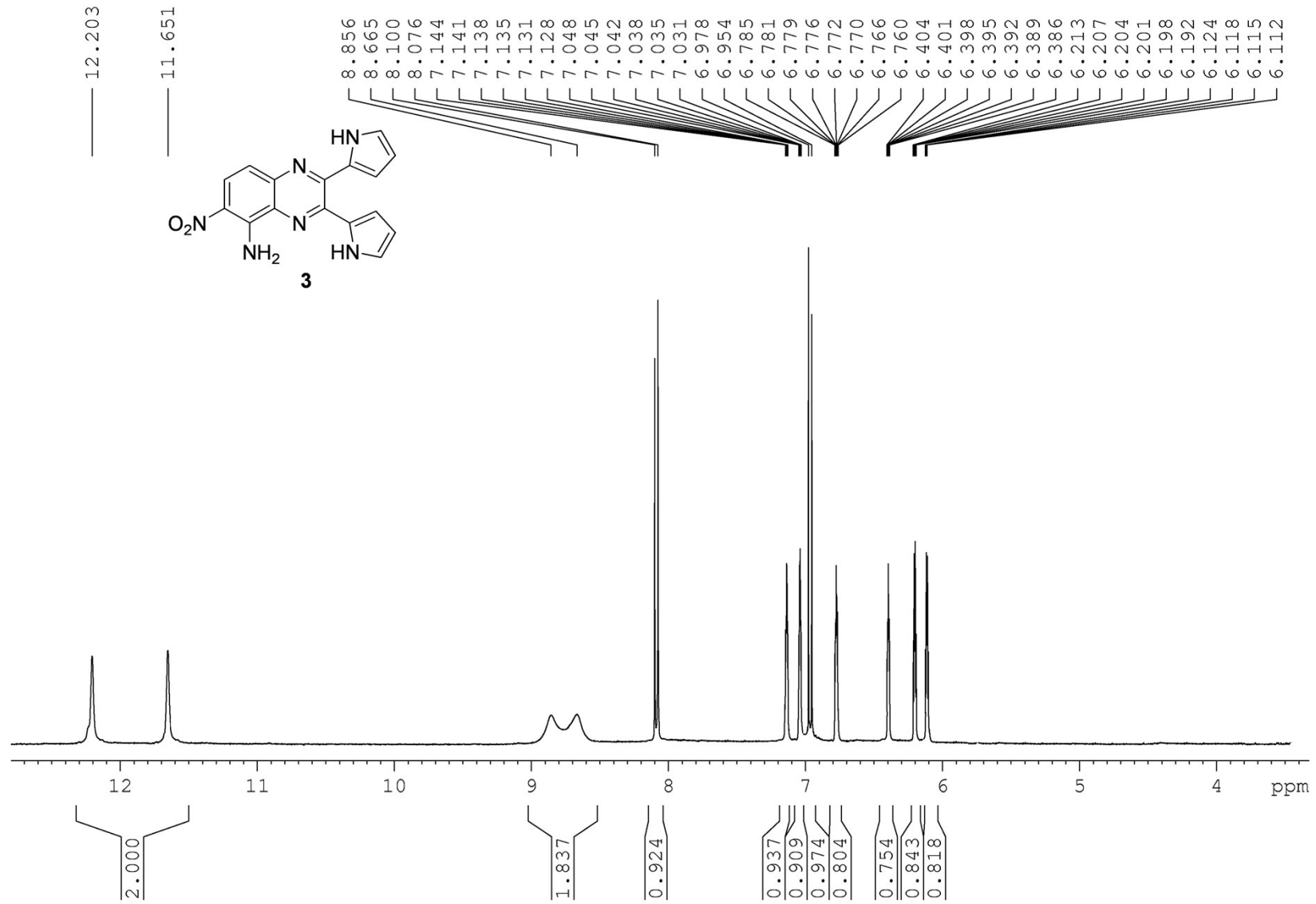

Figure S3. ^{1}H NMR (in DMSO-d_6) spectrum of **3** monitored at 400 MHz.

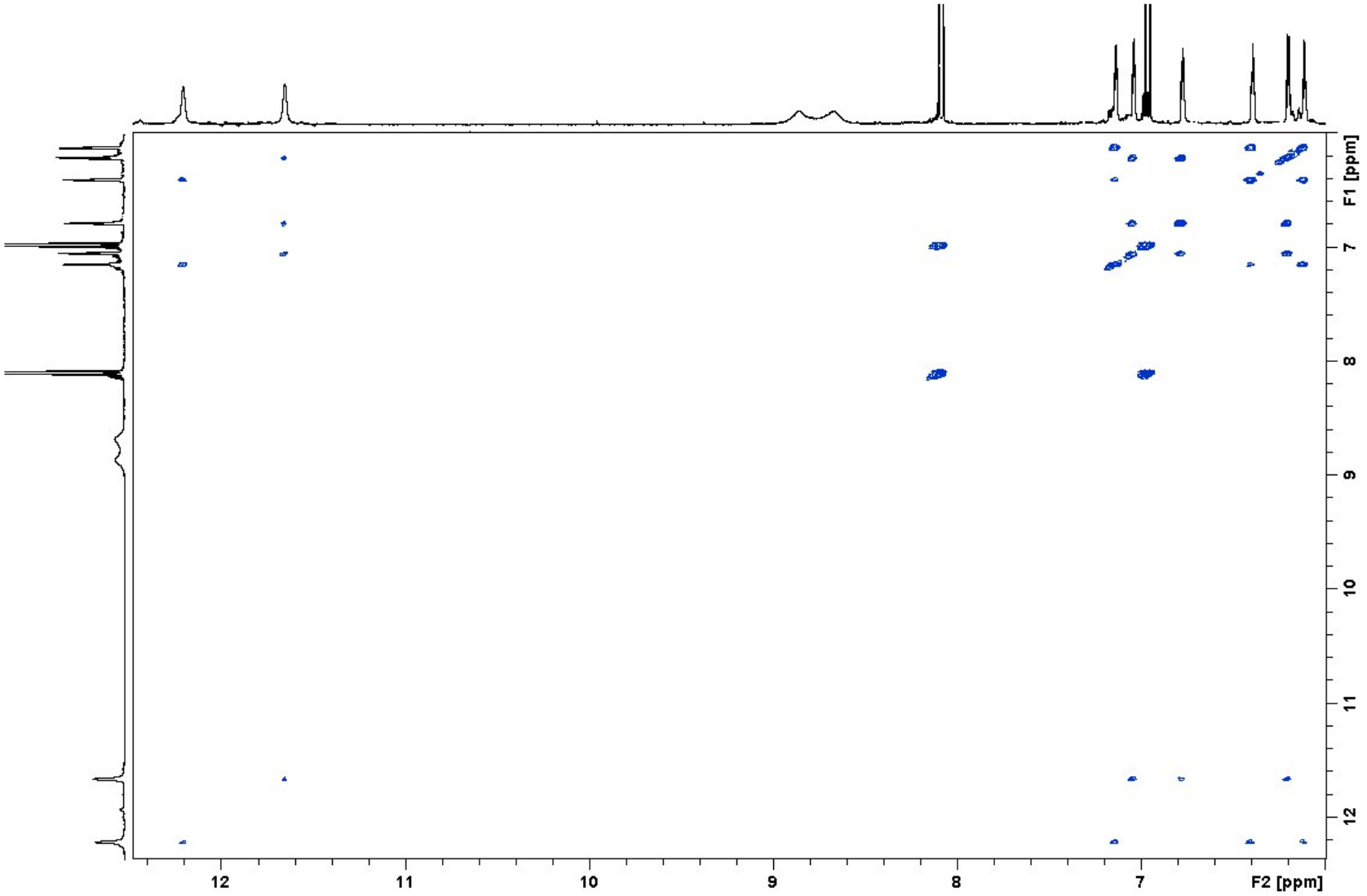

Figure S4. 2D COSY NMR (in DMSO-d_6) spectrum of **3** monitored at 400 MHz.

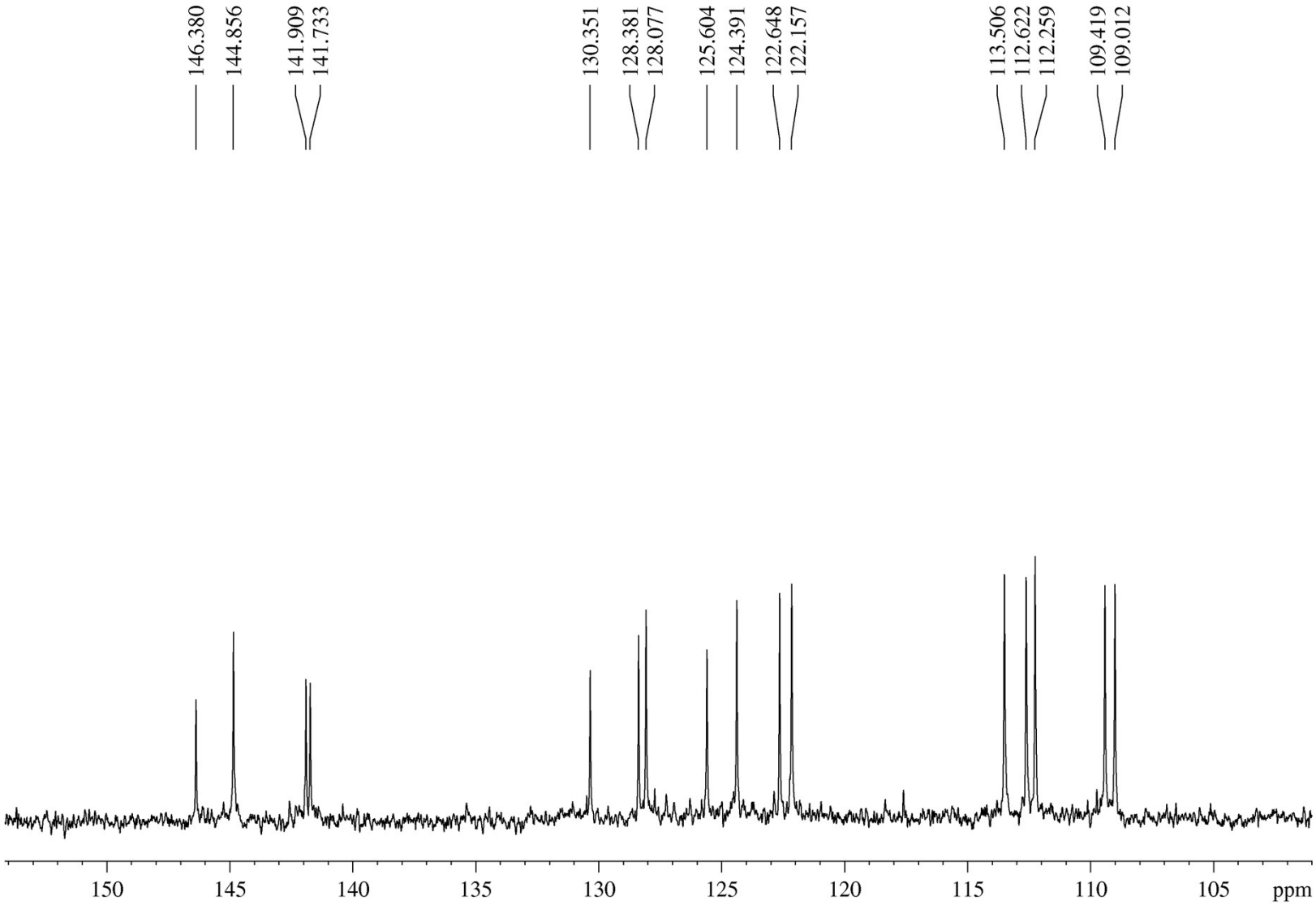

Figure S5. ^{13}C NMR (in DMSO-d_6) spectrum of **3** monitored at 400 MHz.

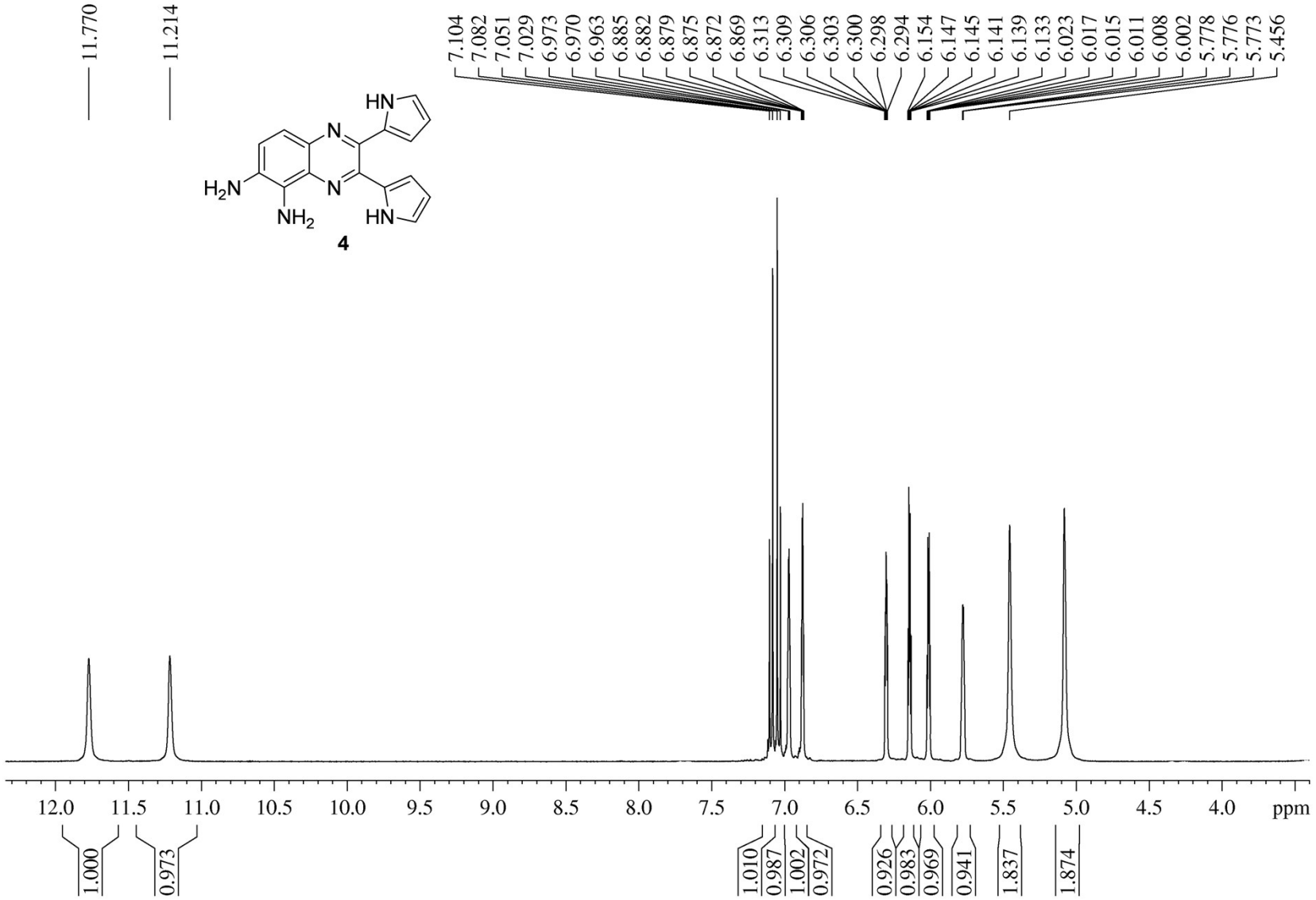

Figure S6. ^{1}H NMR (in DMSO-d_6) spectrum of **4** monitored at 400 MHz.

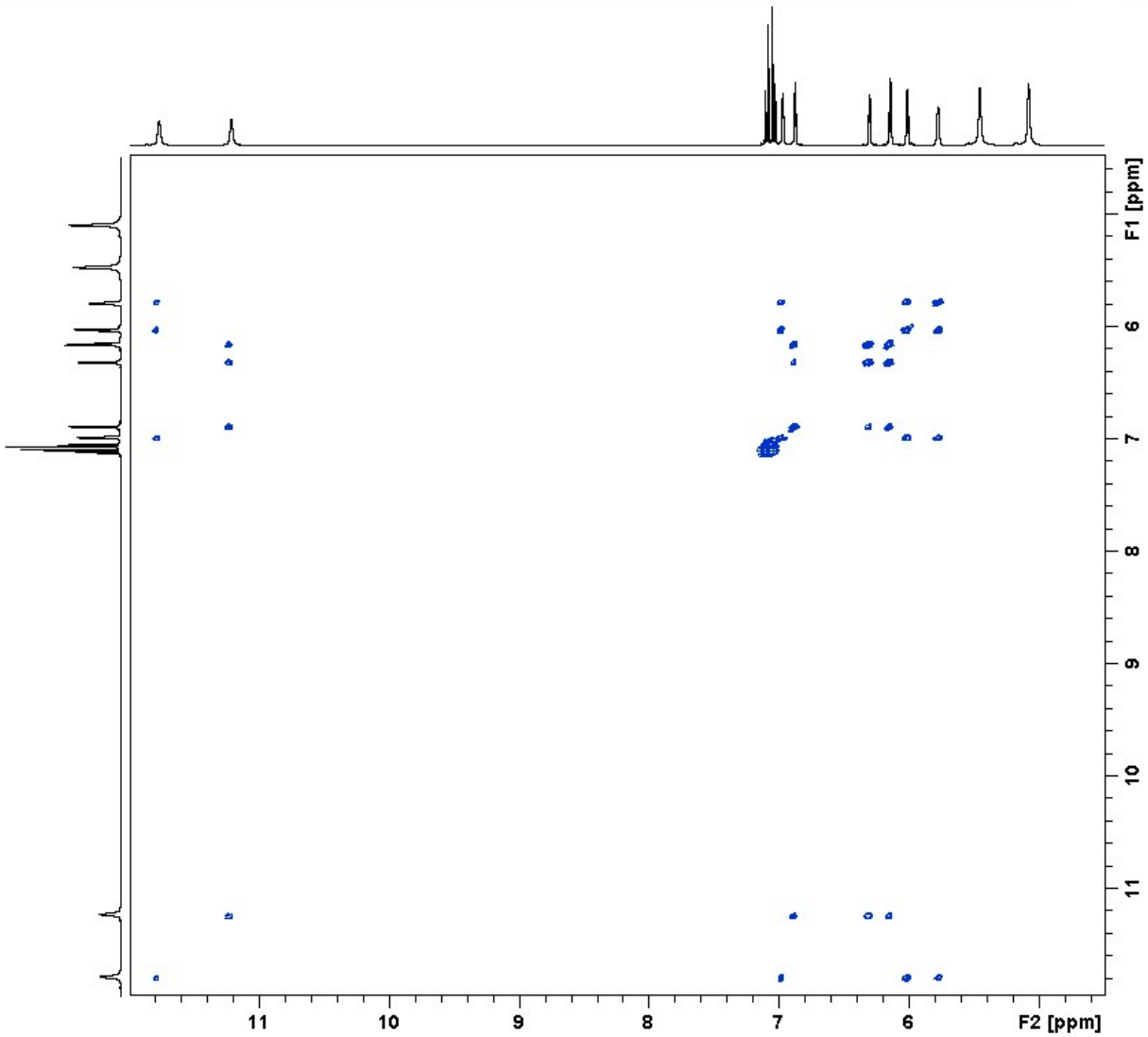

Figure S7. 2D COSY NMR (in DMSO-d_6) spectrum of **4** monitored at 400 MHz.

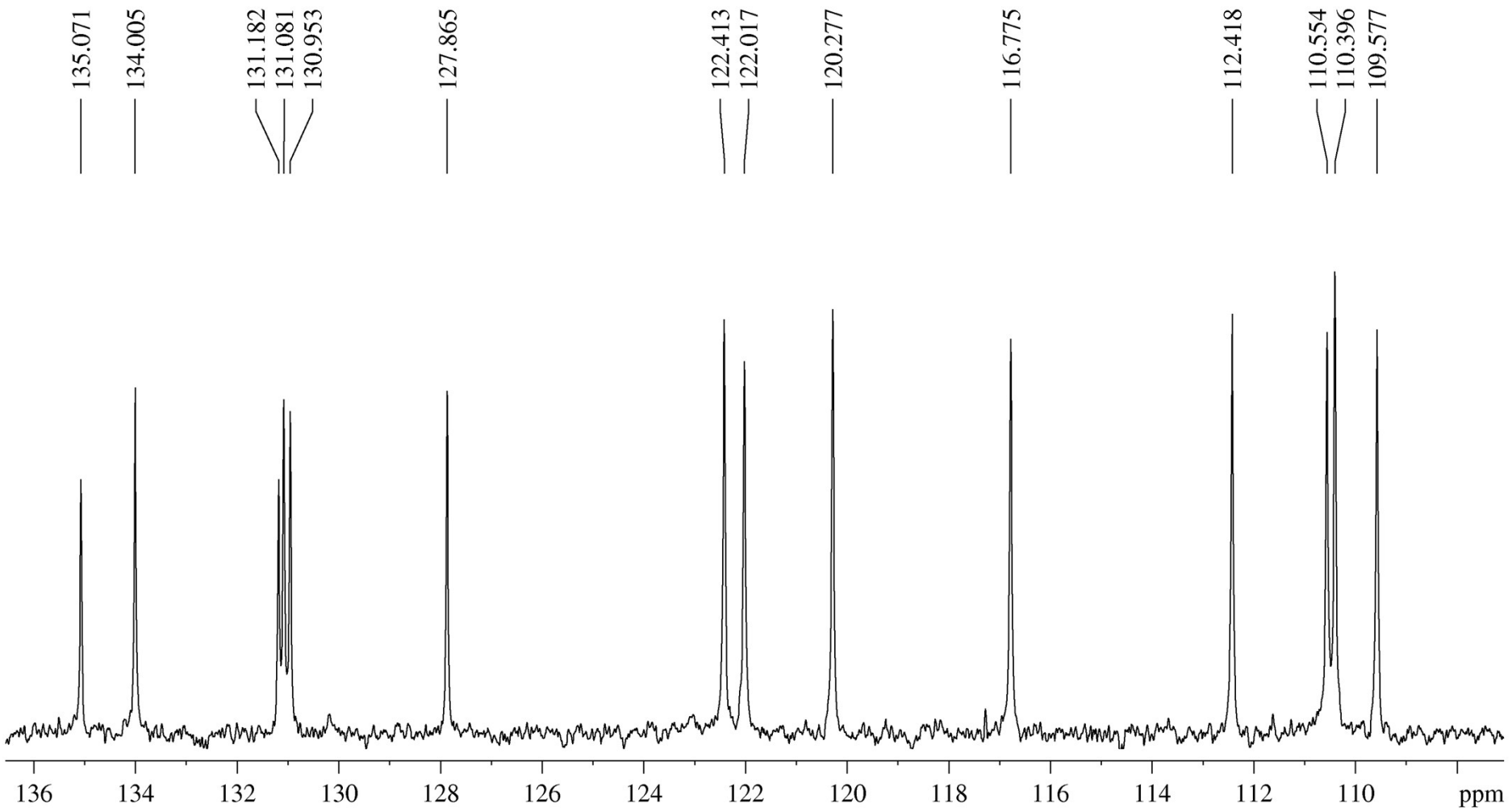

Figure S8. ^{13}C NMR (in DMSO-d_6) spectrum of **4** monitored at 400 MHz.

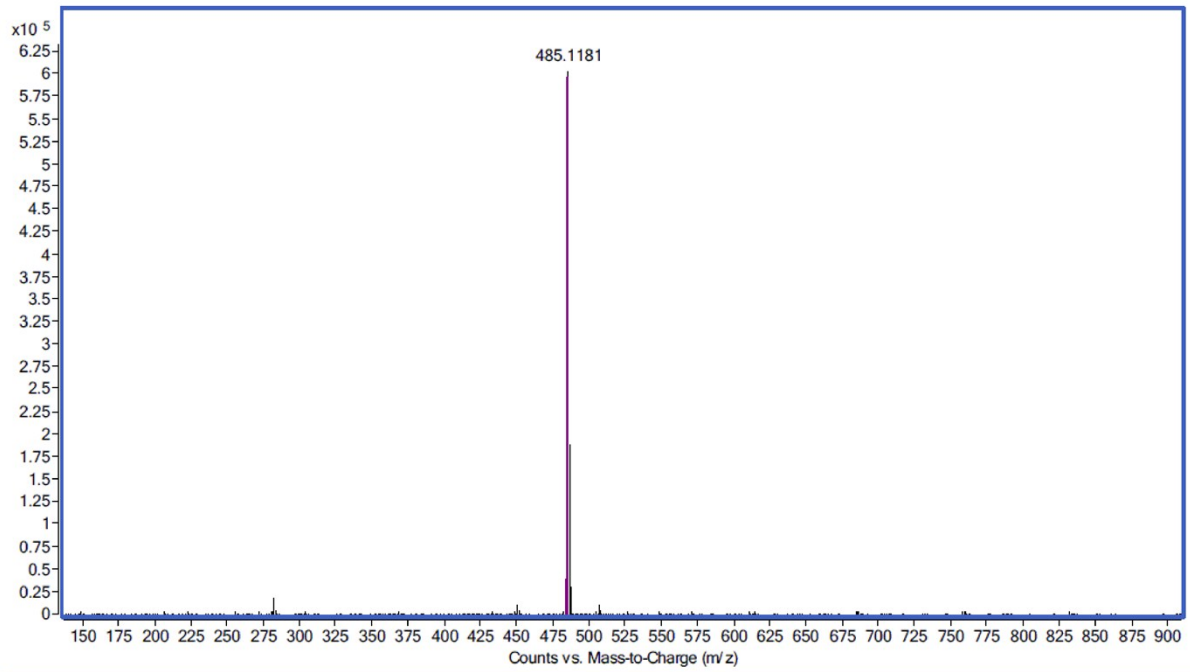

MS Formula Results: + Scan (0.323-0.453 min)

m/z	Ion	Formula	Abundance
483.1234	(M+H)+	C27 H21 Fe N6	31594.6

Best	Formula (M)	Ion Formula	Calc m/z	Score	Mass	Calc Mass	Diff (ppm)
☑	C27 H20 Fe N6	C27 H21 Fe N6	483.1218	64.93	482.1155	482.1146	-1.87

Isotope	Abund%	Calc Abund%	Calc Abund	m/z	Calc m/z	Diff (ppm)	Abund Su
1	5.25	6.35	5.86	483.1234	483.1218	-3.26	4.89
2	2.06	2.01	1.85	484.1237	484.1248	2.27	1.92
3	100	100	92.29	485.1181	485.1172	-1.86	93.19

Figure S9. HRMS-ESI spectrum of **1** in $CHCl_3$ solution.

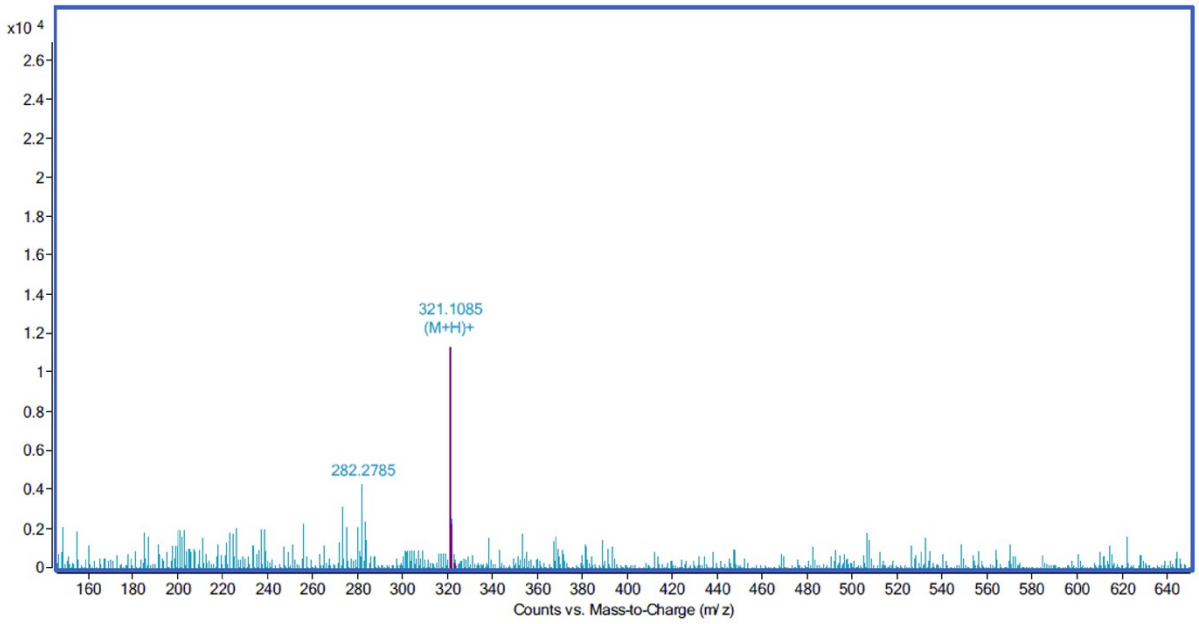

MS Formula Results: + Scan (0.290-0.513 min)

m/z	Ion	Formula	Abundance
321.1085	(M+H)+	C16 H13 N6 O2	10912.6

Best	Formula (M)	Ion Formula	Calc m/z	Score	Mass	Calc Mass	Diff (ppm)
☑	C16 H12 N6 O2	C16 H13 N6 O2	321.1095	94.81	320.1012	320.1022	3.1

Isotope	Abund%	Calc Abund%	Calc Abund	m/z	Calc m/z	Diff (ppm)	Abund Su
1	100	100	81.98	321.1085	321.1095	3.09	79.26
2	22.54	19.72	16.17	322.1112	322.1121	2.99	17.86
3	3.63	2.26	1.85	323.1127	323.1146	5.71	2.88

Figure S10. HRMS-ESI spectrum of **3** in $CHCl_3$ solution.

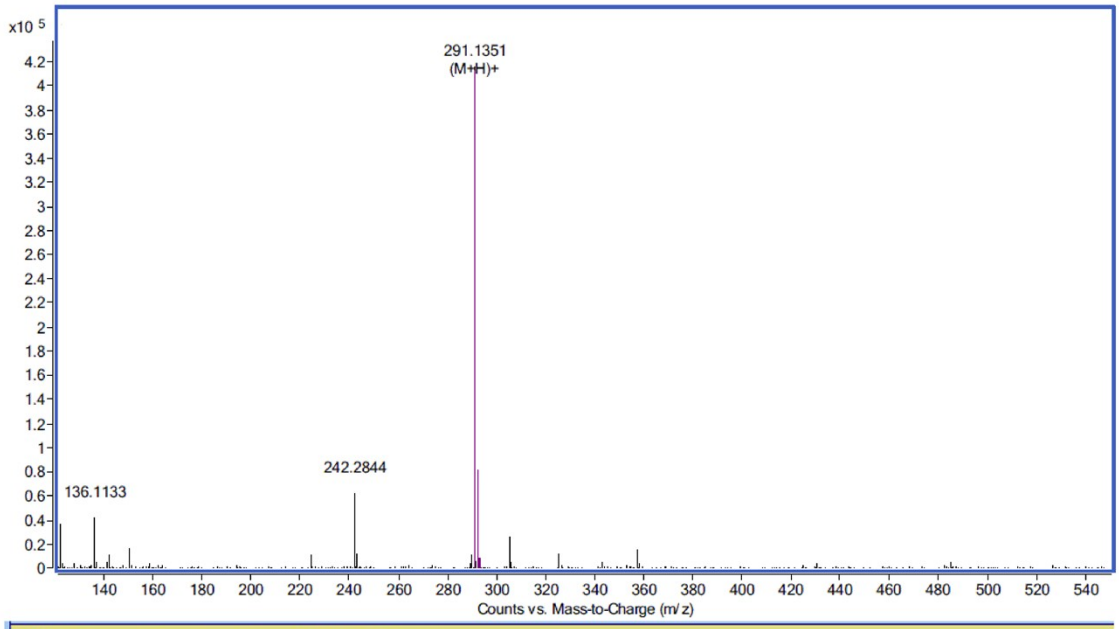

MS Formula Results: + Scan (0.354-0.386 min)

m/z	Ion	Formula	Abundance
291.1351	(M+H)+	C16 H15 N6	415584.8

Best	Formula (M)	Ion Formula	Calc m/z	Score	Mass	Calc Mass	Diff (ppm)
☑	C16 H14 N6	C16 H15 N6	291.1353	99.58	290.1278	290.128	0.54

Isotope	Abund%	Calc Abund%	Calc Abund	m/z	Calc m/z	Diff (ppm)	Abund Su
1	100	100	82.3	291.1351	291.1353	0.54	83.1
2	18.55	19.67	16.19	292.1376	292.1379	1.07	15.42
3	1.78	1.84	1.51	293.1406	293.1406	-0.19	1.48

Figure S11. HRMS-ESI spectrum of **4** in $CHCl_3$ solution.

2. Titration experimental data of anions and cations.

2.1. Electrochemical titrations.

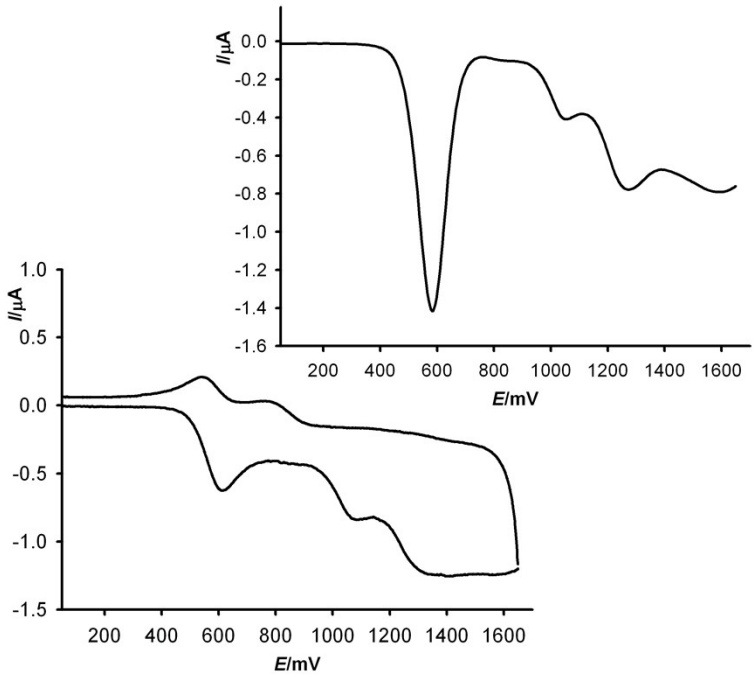

Figure S12. OSWV (top) and CV (bottom) of compound **1** ($1 \cdot 10^{-3}$ M) in CH_3CN using [(*n*-$Bu)_4N]ClO_4$ as supporting electrolyte.

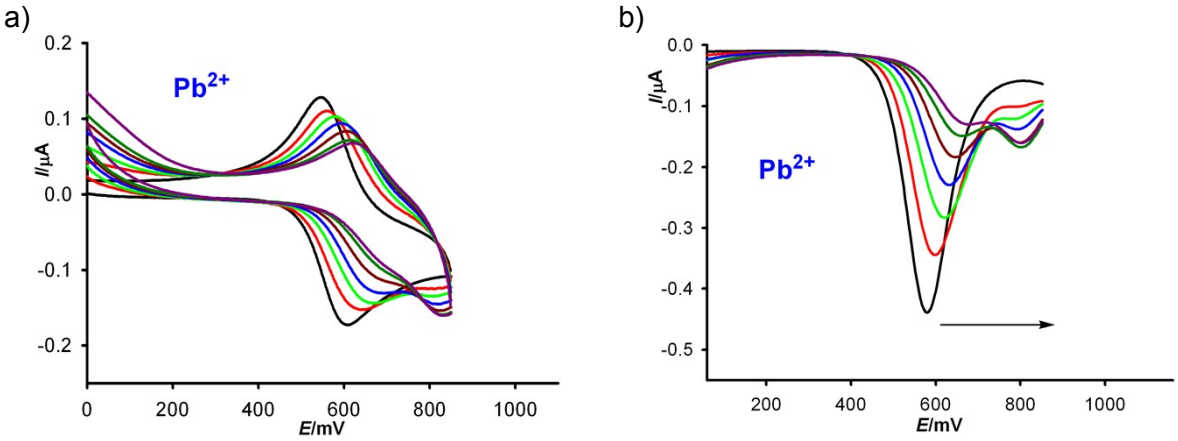

Figure S13. Evolution of the CV (a) and OSWV (b) of **1** (c = 2×10^{-4} M in CH_3CN), using *n*-Bu_4NClO_4 as supporting electrolyte and scanned at 0.1 V s^{-1}, upon addition of increasing amounts of $Pb(ClO_4)_2$.

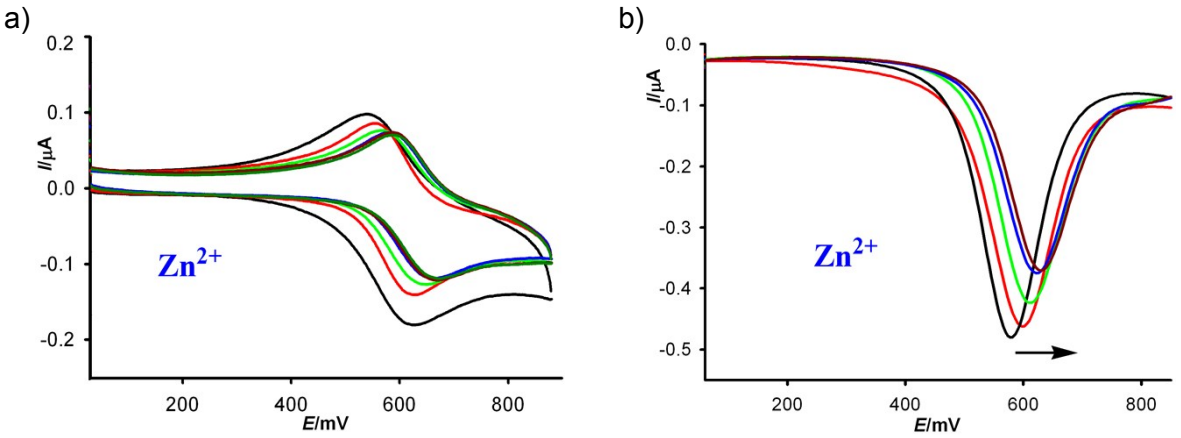

Figure S14. Evolution of the CV (a) and OSWV (b) of **1** (c = $2x10^{-4}$ M in CH_3CN), using *n*-Bu_4NClO_4 as supporting electrolyte and scanned at 0.1 V s^{-1}, upon addition of increasing amounts of $Zn(OTf)_2$.

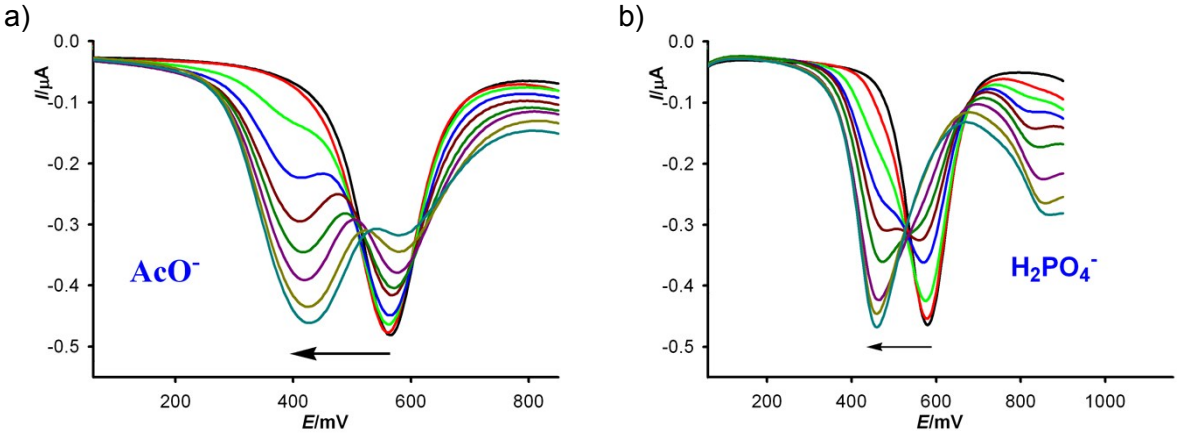

Figure S15. Evolution of the OSWV of **1** (c = $2x10^{-4}$ M in CH_3CN), using *n*-Bu_4NClO_4 as supporting electrolyte and scanned at 0.1 V s^{-1}, upon addition of increasing amounts of: (a) [(*n*-Bu)$_4$N]AcO; (b) [(*n*-Bu)$_4$N]H_2PO_4.

2.2. UV-Vis titration.

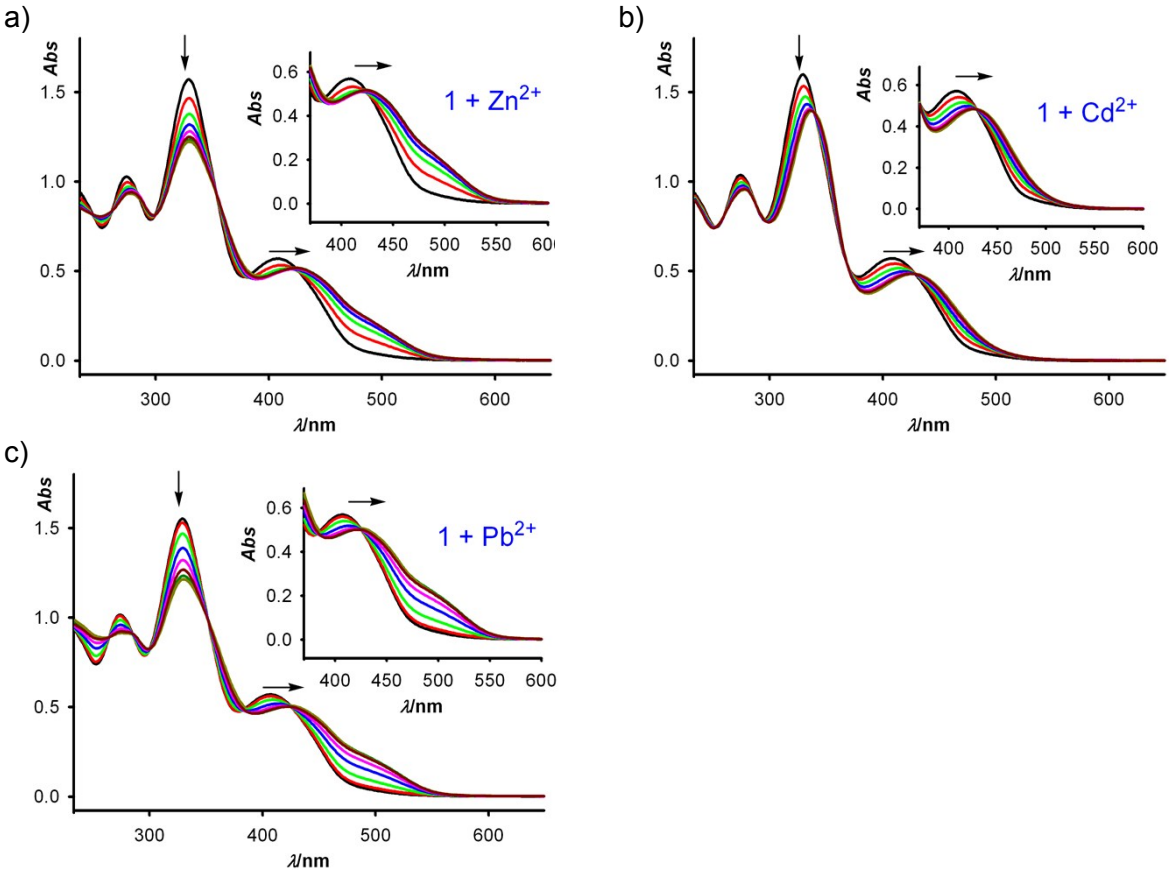

Figure S16. Changes in the absorption spectrum of **1** ($5 \cdot 10^{-5}$ M) upon addition of increasing amounts of (a) $Zn(OTf)_2$; (b) $Cd(ClO_4)_2$;and (c) $Pb(ClO_4)_2$ $_2$ in CH_3CN solution.

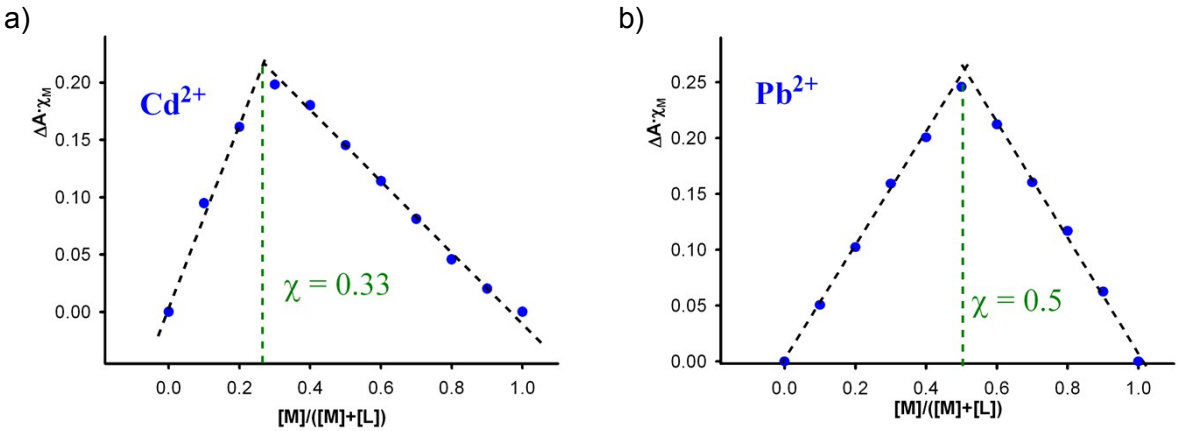

Figure S17. Job's plot obtained upon addition of the appropriate metal cation to **1** ($5x10^{-5}$ M in CH_3CN): (a) $Cd(ClO_4)_2$; (b) $Pb(ClO_4)_2$; (c) $Zn(OTf)_2$.

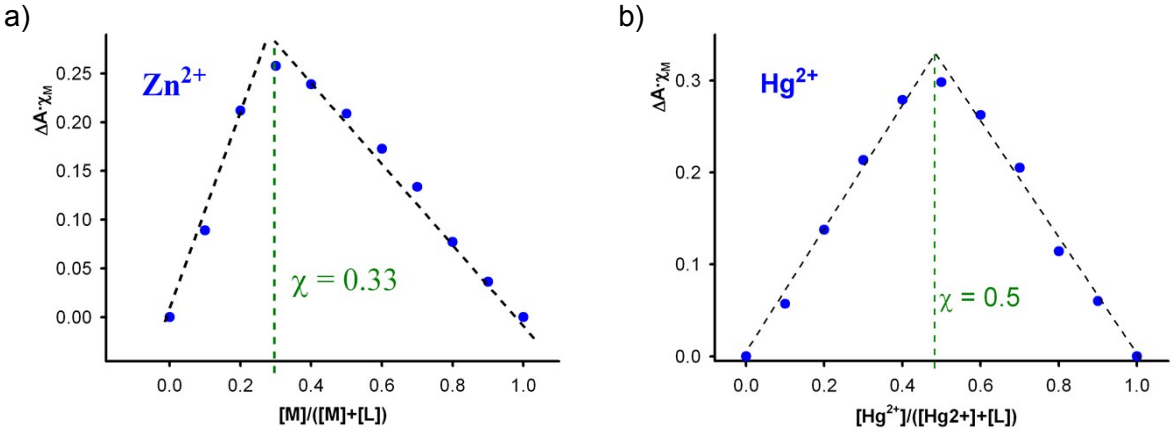

Figure S18. Job's plot obtained upon addition of the appropriate metal cation to **1** ($5x10^{-5}$ M in CH_3CN): (a) $Zn(OTf)_2$ ($5x10^{-5}$ M in MeCN); (b) $Hg(OTf)_2$ ($5x10^{-5}$ M in MeOH or CH_3CN).

Tabla S1. UV-Vis data of receptor 1 MeOH solution.

Compound	Solvent	λ/nm (10^{-4}ε, $M^{-1}cm^{-1}$)	PI (nm)
1	MeOH	275 (1.431); 325 (1.873); 413 (0.825)	--
1+ Hg^{2+}	MeOH	285 (1.190); 335 (1.334); 445 (0.606)	345; 385

2.3. ESI-MS.

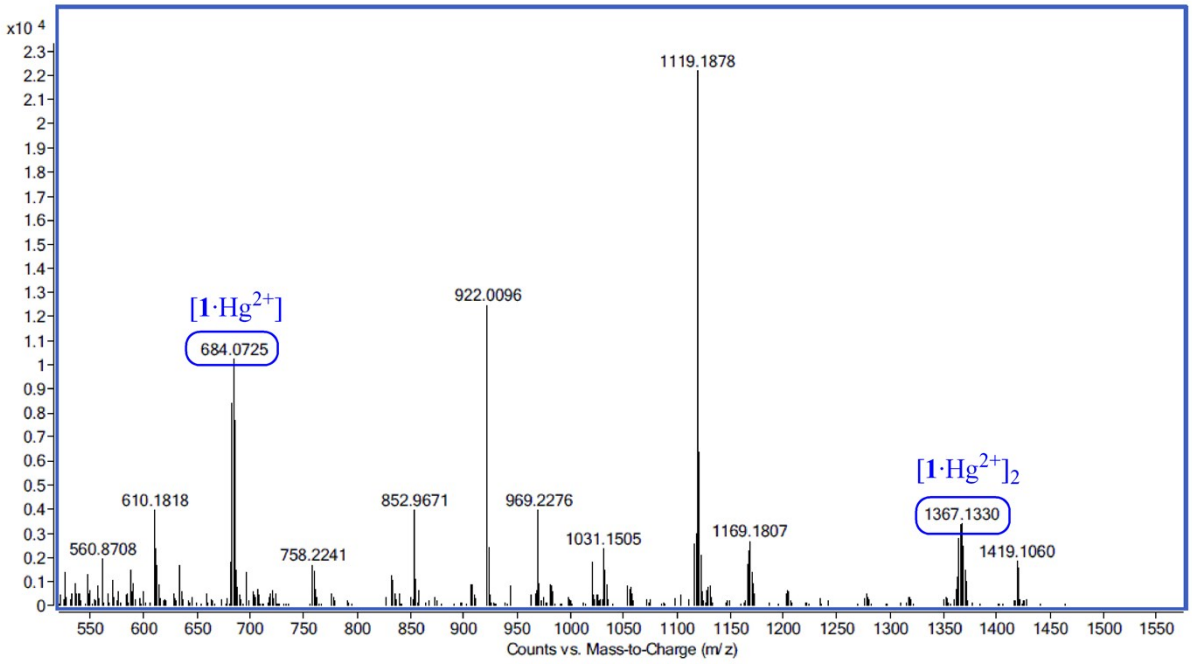

Figure S19. ESITOF mass spectrum of an CH_3CN solution of **1** in the presence of an equimolecular amount of $Hg(OTf)_2$.

2.4. Fluorescence emission titrations.

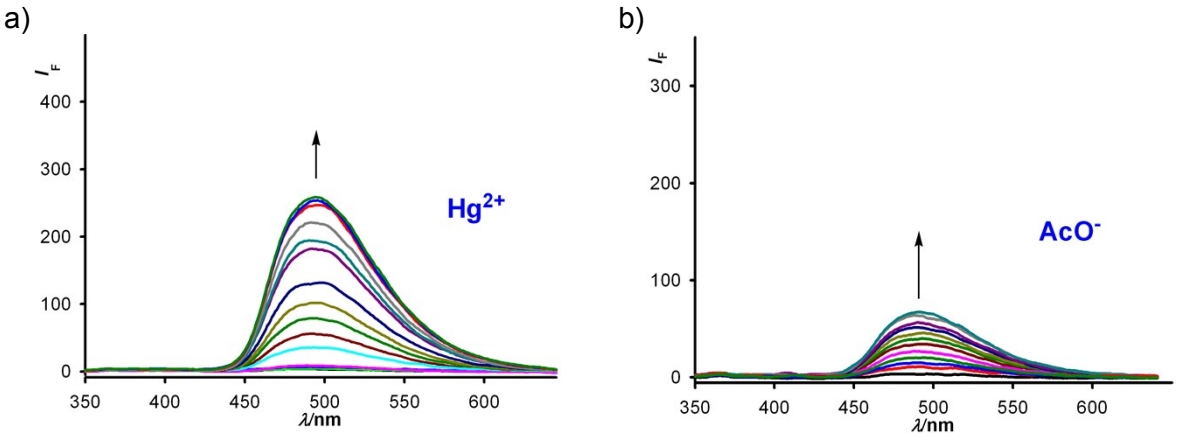

Figure S20. Changes in the emission spectrum of **1** (c = $1 \cdot 10^{-5}$ M) in CH_3CN upon addition of: (a) $Hg(OTf)_2$; (b) $[(n\text{-}Bu)_4N]AcO$ Emission is monitored at λ_{exc} = 330 nm.

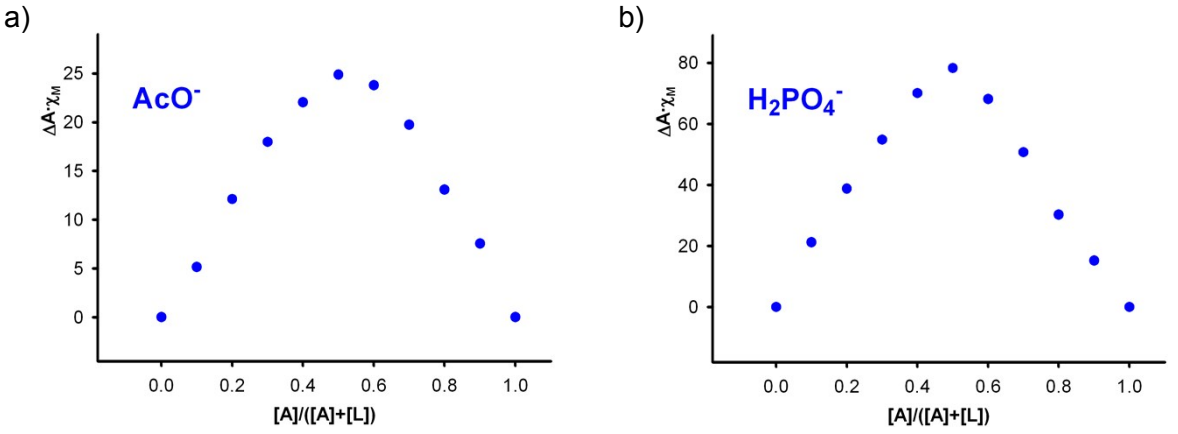

Figure S21. Job's plot obtained upon addition of the appropriate anion to **1** (1×10^{-5} M in CH_3CN): (a) $[(n\text{-}Bu)_4N]OAc$; (b) $[(n\text{-}Bu)_4N]H_2PO_4$.

3. Titration experimental data of ion pairs.

3.1. UV-Vis titrations.

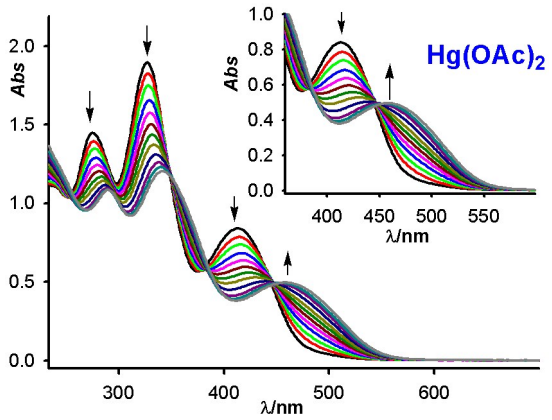

Figure S22. Changes in the absorption spectrum of **1** (c = $5 \cdot 10^{-5}$ M in CH_3OH) upon addition of increasing amounts of $Hg(OAc)_2$; until 2 equiv were added. Arrows indicate absorptions that increase or decrease during the experiment.

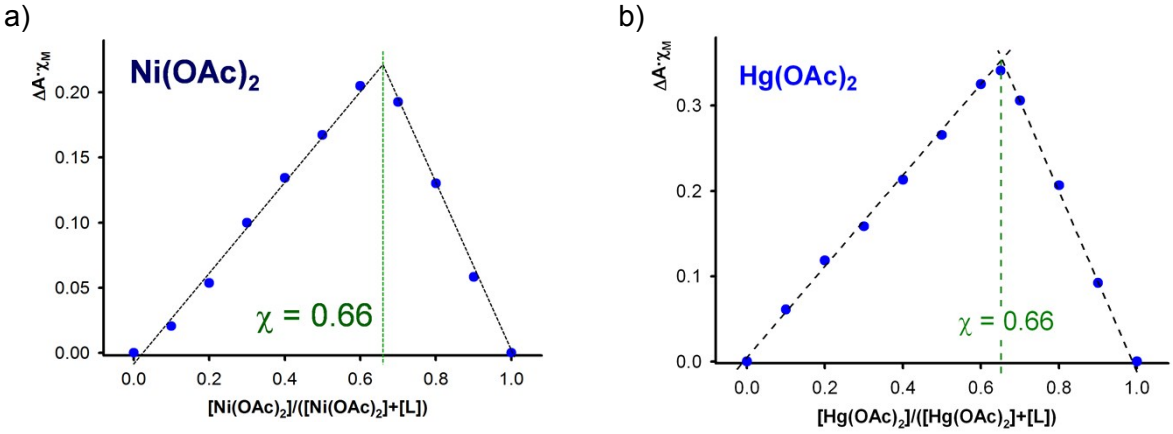

Figure S23. Job's plot obtained upon addition of the appropriate metal cation to **1** (5×10^{-5} M in CH_3CN): (a) $Ni(OAc)_2$; (b) $Hg(OAc)_2$ (5×10^{-5} M in CH_3CN).

Tabla S2. UV-Vis data of receptor 1 in MeOH solution.

Compound	λ/nm (10^{-4}ε, $M^{-1}cm^{-1}$)	PI (nm)	K (M^{-2})
1	275 (1.431); 325 (1.873); 413 (0.825)		
1+Hg(AcO)$_2$	290 (1.100); 345 (1.170); 467 (0.508)	345; 445	$3.13 \cdot 10^{10}$

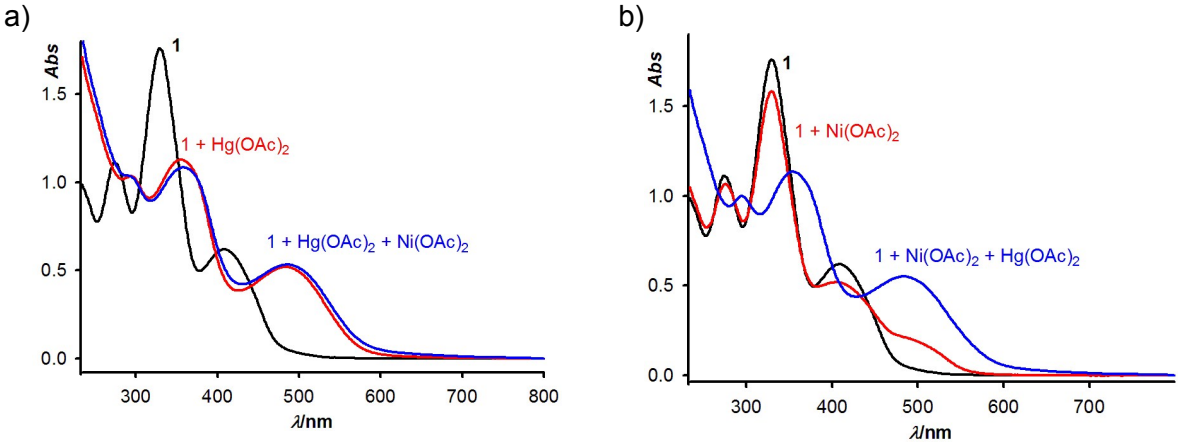

Figure S24. (a) UV-vis spectrum of receptor **1** (black line) after addition of $Hg(OAc)_2$ (red line) and after simultaneous addition of $Ni(OAc)_2$ to the preformed complex [**1**·$[Hg(OAc)_2]_2$] (blue line). (a) UV-vis spectrum of receptor **1** (black line) after addition of $Ni(OAc)_2$ (red line) and after simultaneous addition of $Hg(OAc)_2$ to the preformed complex [**1**·$Ni(OAc)_2$] (blue line).

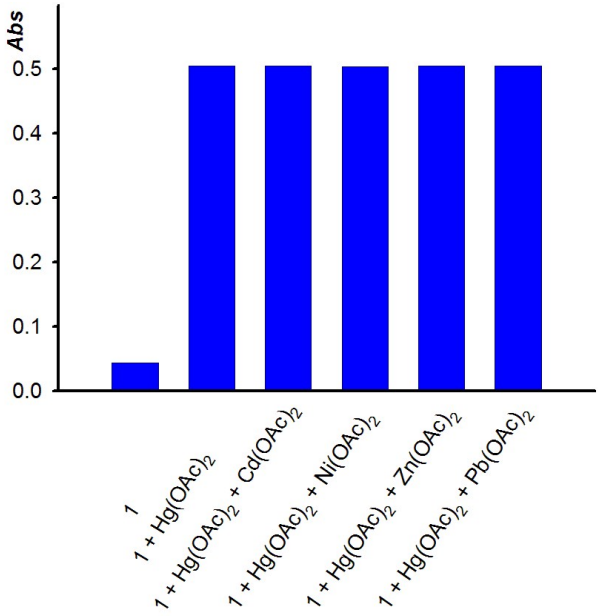

Figure S25. Absorption intensity of **1** upon addition of 2 equiv of $Hg(OAc)_2$ in the presence of 2 equiv of interference ion-pairs in MeCN solution.

3.2. ^{1}H RMN titrations data.

Table S3. ^{1}H RMN titrations data.

	NH_{im}	$NH_{1'}$	$NH_{1''}$	H_α	H_β	H_{Cp}
1	10.66	9.66	9.39	5.01	4.47	4.14
1+AcO$^-$	--	9.62 (-0.04)	12.12 (2.73)	5.46 (0.45)	4.32 (-0.15)	4.07 (-0.07)
1+Hg^{2+}	12.93 (2.27	10.96 (1.3)	10.14 (0.75)	5.25 (0.24)	4.55 (0.08)	4.12 (-0.02)
1+Hg(OAc)$_2$	12.35 (1.69)	10.79 (1.13)	9.81 (0.42)	5.33 (0.32)	4.68 (0.21)	4.24 (0.1)

	H_8	H_7	$H_{5'}$	$H_{5''}$	$H_{3''}$	$H_{3'}$	$H_{4''}$	$H_{4'}$
1	7.98	7.77	7.01	6.95	6.91	6.64	6.33	6.27
1+AcO$^-$	7.85 (-0.13)	7.58 (-0.19)	6.93 (-0.08)	6.61 (-0.34)	7.03 (0.12)	6.93 (0.29)	6.07 (-0.26)	6.23 (-0.04)
1+Hg^{2+}	7.69 (-0.29)	7.62 (-0.15)	7.04 (0.03)	6.69 (-0.26)	7.12 (0.21)	7.09 (0.45)	6.13 (-0.20)	6.28 (0.01)
1+Hg(OAc)$_2$	7.80 (-0.18)	7.70 (-0.07)	6.84 (-0.17)	7.15 (0.2)	7.15 (0.24)	7.08 (0.44)	6.32 (-0.01)	6.19 (-0.08)

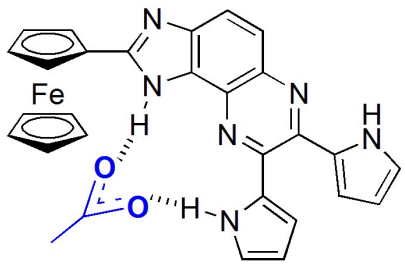

[**1**·AcO$^-$]

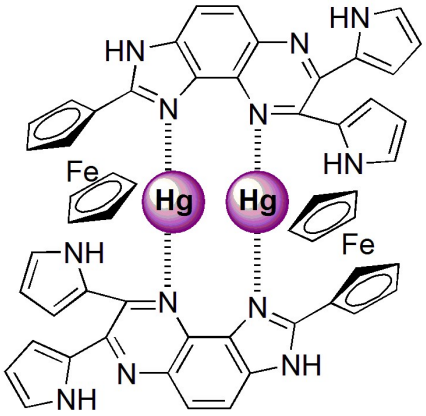

[**1**·Hg^{2+}]$_2$

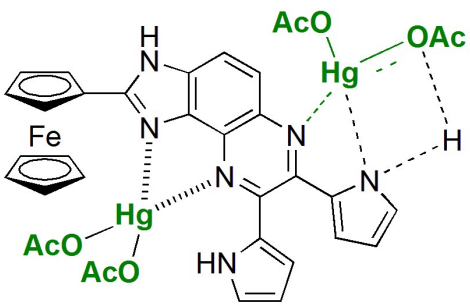

[**1**·[(Hg(OAc)$_2$]$_2$]

Figure S26. Tentative binding modes of the complex formed.